J Mater Sci: Mater Med (2010) 21:1–10
DOI 10.1007/s10856-009-3828-8

The effects of hydroxyl groups on Ca adsorption on rutile surfaces: a first-principles study

Xiong Lu · Hong-ping Zhang · Yang Leng · Liming Fang · Shuxin Qu · Bo Feng · Jie Weng · Nan Huang

Received: 8 May 2009 / Accepted: 14 July 2009 / Published online: 29 July 2009

Abstract Hydroxyl groups on titanium surfaces have been believed to play an important role in absorbing Ca in solution, which is crucial in the formation of bioactive calcium phosphates both in vitro and in vivo. CASTEP, a first-principles density functional theory (DFT) code, was employed to investigate Ca adsorption on various rutile (110) surfaces in order to clarify how hydroxyl groups effect Ca adsorption. The surfaces modeled in the present study include a bare rutile (110) surface, a hydroxylated rutile (110) surface, an oxidized rutile (110) surface, and a rutile (110) surface bonded with mixed OH groups and water. The results reveal that not all OH groups favors to attract Ca adsorption and loosely bonded OH and water on a rutile surface actually combine with Ca during adsorption. An oxidized rutile surface has the highest ability to attract Ca atoms, which partially explains that alkali-treated Ti surfaces could induce hydroxyapatite formation in alkaline environments.

X. Lu · Y. Leng
Department of Mechanical Engineering, Hong Kong University of Science and Technology, Kowloon, Hong Kong, China

X. Lu (✉) · H. Zhang · S. Qu · B. Feng · J. Weng · N. Huang
Key Lab of Advanced Technologies of Materials, Ministry of Education, School of Materials Science and Engineering, Southwest Jiaotong University, Chengdu 610031, China
e-mail: luxiong_2004@163.com

L. Fang
School of Materials Science and Engineering, South China University of Technology, Guangzhou 510641, China

1 Introduction

Titanium and titanium alloy implants have become the most popular biomedical materials due to their biocompatibility, excellent corrosion resistance, good mechanical properties and lightness. Titanium without any surface treatments is bioinert, not bioactive, and cannot form direct bonding with surrounding bone tissues when implanted in the human body. There are numerous studies on Ti surface treatments to enhance its bioactivity. These treatment methods have mainly focused on modifying the outer most atomic layers on a titanium surface, the passive TiO_2 layers, as summarized in our previous paper [1]. An effective approach is the alkali treatment process introduced by Kokubo et al. [2–4]. They demonstrated that alkali-treated Ti can induce calcium phosphate (Ca–P) formation in simulated body fluids (SBF) because alkali treatment can form a Ti–OH layer on titanium surfaces. Then, the Ti–OH groups combine with Ca in SBF to form amorphous calcium titanate; in turn, the calcium titanate combines with the phosphate ions to form amorphous Ca–P that eventually transforms into bone-like apatite for new bone formation. Since the alkaline treatment can convert bioinert titanium into a bioactive material, it is of particular interest to investigate the interaction between Ca and hydroxylated titanium surfaces.

There has been growing recognition that OH groups play an important role in bioactivity because they widely exist on titanium surfaces and have been shown to be directly related to apatite formation [5, 6]. Our recent study demonstrated that a concentrated OH group might not be sufficient for bioactivity and that only those of OH tightly bonded with Ti correlated well with the apatite formation in SBF [7]. We note that experimental studies of OH interactions with Ca using routine techniques are difficult

because these interactions may involve electron transfer at the atomic scale. Computer simulation provides an useful way to study the interactions between Ca and titanium surfaces. In recent years, density functional theory (DFT) calculations have become popular in studying molecular and atomic adsorption on crystal surfaces. DFT does not require empirical parameters, but relies on explicit quantum mechanics treatment of the electrons in a model system by solving Schrodinger's equation indirectly to determine the electronic ground state [8].

In this study, Cambridge Sequential Total Energy Package (CASTEP), a first-principles DFT code, was used to investigate the effects of OH groups on Ca adsorption on rutile surfaces. CASTEP employs the plane-wave pseudopotential method to examine the properties of crystals and surfaces [9]. Rutile is the passive layer on titanium surfaces and has been extensively studied [10–12]. The (110) surface of rutile crystal (hereafter called R(110)) is particularly important since it is widely considered as a model for metal–oxide surfaces [13–17]. Although only a few theoretical studies on the deposition of calcium atoms on rutile surfaces has been reported in the literature, a clear explanation of the role of OH groups during the Ca adsorption process remains to be established [16, 18]. In this study, the adsorption of Ca on four types of rutile surfaces was calculated, including a bare R(110) surface, an R(110) surface covered with OH groups, an R(110) surface covered with oxygen atoms, and an R(110) surface covered with mixed OH groups and water. The adsorption energy, electronic structure and electron transfer during Ca adsorption on different type of hydroxylated R(110) surfaces were compared.

2 Computational details

A rutile (110) surface, which is the most thermodynamically stable crystallographic surface of stoichiometric rutile, has a corrugated form as shown in Fig. 1a and b. The lattice parameters for the surface slab used in our computations are 5.935 Å × 6.597 Å × 4.573 Å. The surfaces contain fivefold (5f) and sixfold (6f) Ti atoms and two types of surface oxygen atoms, referred to as bridging and in-plane oxygen atoms, as indicated in Fig. 1a [19]. The bridging oxygen atoms sit above the 6f-Ti and the in-plane oxygen atoms bond to three Ti atoms in the plane. There are 14 O and 8 Ti atoms in the model. This model contains all the typical features of the well-understood rutile (110) surface that has been widely used in the literature [19, 20]. A periodic boundary condition was used to model this slab and a 20 Å vacuum was added on the slab to ensure that Ca did not interact with the images of the slab in the neighboring cells. Four types of rutile surfaces were considered as follows.

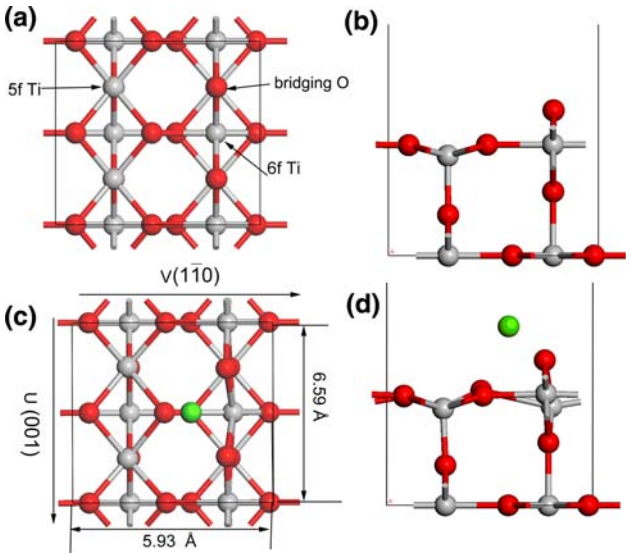

Fig. 1 **a** Top view of the stoichiometric rutile (110) surface after geometric optimization. The fivefold and sixfold coordinated Ti and the bridging oxygen atoms are labeled as 5f-Ti, 6f-Ti and bridging O, respectively; **b** Side view of (**a**); **c** Top view of Ca adsorption on the surface; **d** Side view of (**c**). Ti, grey; O, red; Ca, green; H, white. The color code is the same in the following figures. (Color figure online)

Case (1): Bare R(110) relaxed surfaces as shown in Fig. 1: the position of the in-plane oxygen atoms is slightly higher than that of 5f-Ti after relaxation.

Case (2): Hydroxylated rutile (110) surfaces: a Ti–O bond is formed between the OH groups and the 5f-Ti through an oxygen atom (O_{OH}). An H–O bond is formed between the hydrogen atom and the bridging oxygen atom (Fig. 2). Hence, the whole surface is covered with hydroxyl groups. This surface represents cases when the Ti surface has been alkali treated with saturated OH groups.

Case (3): Oxidized rutile (110) surfaces: All the hydrogen atoms in Case 2 are removed and only oxygen atoms remain (Fig. 3). This surface represents cases when alkali-treated Ti is soaked in an alkali solution, such as simulated body fluid, and the OH groups are deprotonated to expose pure oxygen atoms on the surfaces.

Case (4): R(110) bonded with mixed OH groups and water: one of the hydroxyl groups grafted onto Ti in Case 2 is replaced by an H_2O molecule (Fig. 4). Specifically, the oxygen atom in water (O_{water}) is bonded to one of the 5f-Ti (Ti4) atoms and one hydroxyl group is bonded to the other 5f-Ti (Ti3). This surface represents the cases when not all water molecules are dissociated into H and OH groups, and the OH and water may coexist on the surface of the titanium oxide. This model with mixed OH and water has been proved to be energetically stable [13, 21]. It should be mentioned that another possibility where the water bonds to the 6f-Ti between two bridging oxygen atoms was found to be extremely unstable [20].

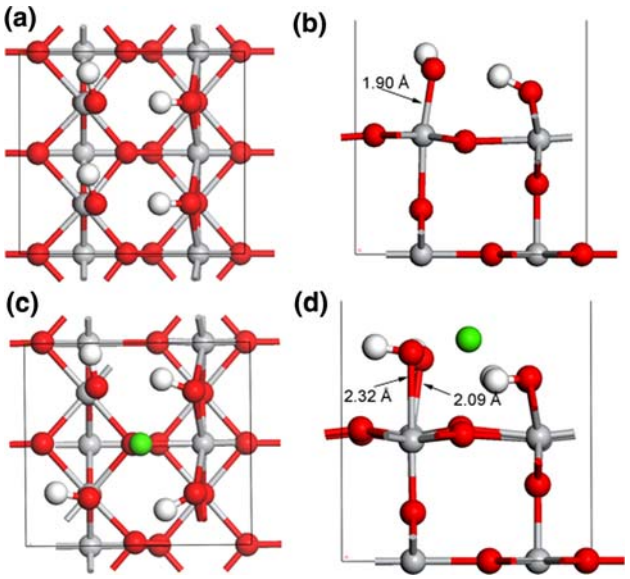

Fig. 2 **a** Top view of the R(110) surface covered with hydroxyl groups after geometric optimization; **b** Side view of (**a**); **c** Top view of Ca adsorption on the surface; **d** Side view of (**c**)

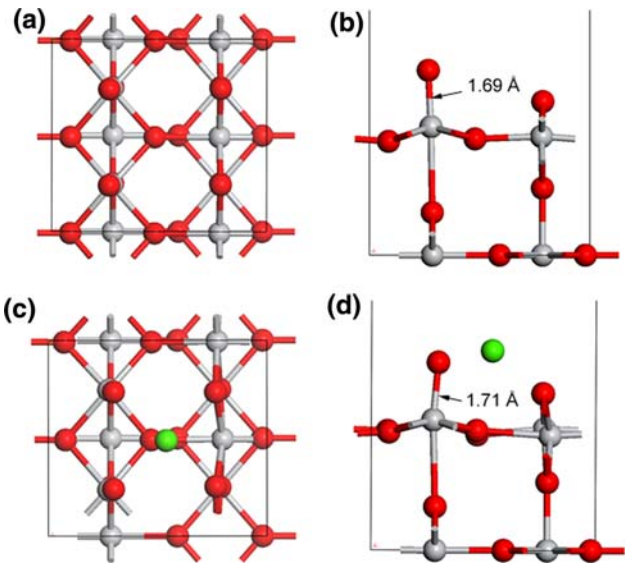

Fig. 3 **a** Top view of the oxidized R(110) surface after geometric optimization; **b** Side view of (**a**); **c** Top view of Ca adsorption on the surface; **d** Side view of (**c**)

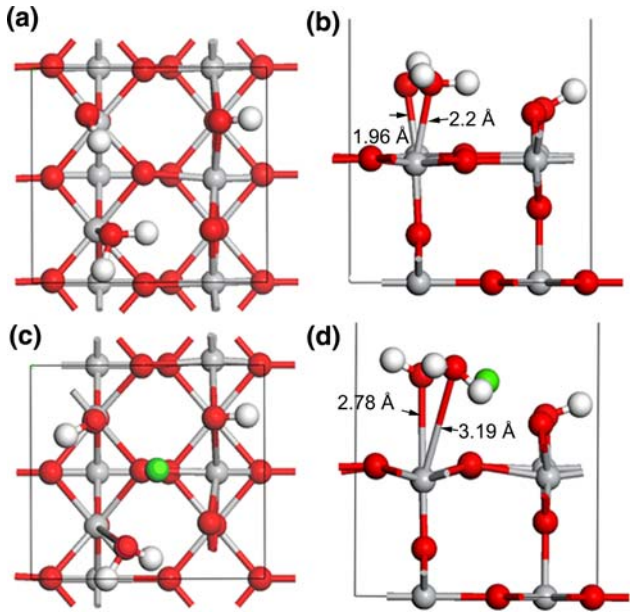

Fig. 4 **a** Top view of the R(110) surface bonded with OH groups and water molecules. One of the hydroxyl groups binding to 5f-Ti was replaced by a H_2O molecule. **b** Side view of (**a**); **c** Top view of Ca adsorption on the surface; **d** Side view of (**c**)

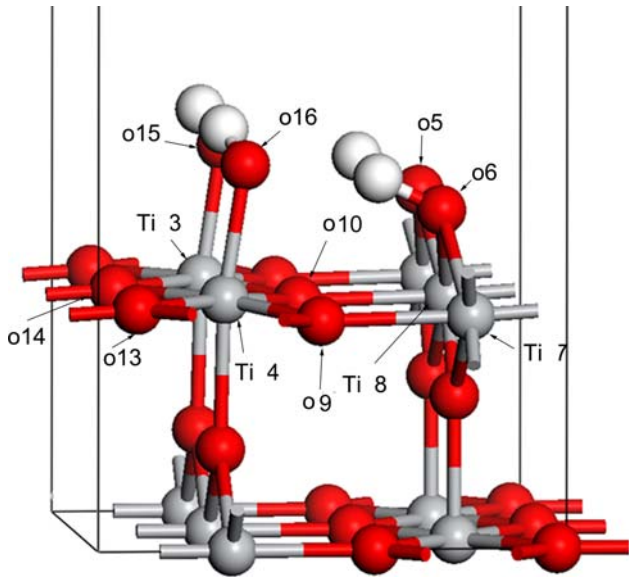

Fig. 5 The atom names used in the calculation

The atoms used in the calculations are shown in Fig. 5. All four surface models were equilibrated after an optimization process and then the Ca atoms were added on the pre-optimized surfaces followed by a new optimization process to obtain an equilibrium state. The models shown in Figs. 1, 2, 3, 4 are in equilibrium after geometric optimization and the detailed optimization conditions and the convergence criteria are presented in the next section. During the optimization process, Ca and the upper atomic layer of the surface were allowed to fully relax in all of the calculations while the atoms in the bottom layer were kept fixed. Fixing the lower layers of atoms is a commonly used method to simplify the process of the adsorption of ions on surfaces for the sake of reducing computational cost [22, 23]. During the calculation, it was also found that only the OH group on the top layer was affected by the Ca atoms. The in-plane O and Ti atoms at the surface did not move in a large range, which showed that the fixation of

the bottom layer was reasonable. The covalent bond strength between the Ca atom and the rutile surface was estimated by calculating the electron bond populations by projecting the plane-wave states onto the localized basis set by means of Mulliken electron population analysis [24].

The first-principles quantum mechanics calculations were run using the CASTEP module in Materials Studio (Accelrys, San Diego, CA). The valence states taken into account in our calculations were Ca-$3s^2 3p^6 4s^2$, Ti-$3s^2 3p^6 3d^2 4s^2$ and O-$2s^2 2p^4$. CASTEP uses Vanderbilt-type ultrasoft pseudopotentials, which allow calculations to be performed with the lowest possible cutoff energy for the plane-wave basis set. The value of the $dE_{tot}/dlnE_{cut}$ gives a good indication of the convergence of the calculation with respect to the cut-off energy. A value of 0.1 eV/atom for *dE* is sufficient for most calculations. When the cut-off energy was set to 340 eV, the *dEs* of O, H, Ca, and Ti in the system were smaller than 0.1 eV/atom according to the convergence test. Thus, in the present study, the plane-wave basis set had a cutoff energy of 340 eV, which is sufficient to lead to good convergence for total energy calculations of the atoms [25]. The exchange-correlation energy was calculated using the Perdew–Burke–Ernzerhof (PBE) generalized gradient approximation (GGA). Special points sampling integration over the Brillouin zone was employed by using the Monkhorst–Pack schemes with a $4 \times 4 \times 1$ *k*-point mesh resulting in 8 *k*-points in the irreducible part of the Brillouin zone [26]. The structure was optimized with the Broyden–Fletcher–Goldfarb–Shanno (BFGS) method and the convergence criteria for the geometric optimization and energy calculation were set to: (a) a self-consistent field tolerance of 1.0×10^{-6} eV/atom; (b) an energy tolerance of 1.0×10^{-5} eV/atom; (c) a maximum force tolerance of 0.03 eV/Å; (d) a maximum displacement tolerance of 1.0×10^{-3} Å. The selection of these parameters was justified by performing tests on the stability of the structure and relative energies as the accuracy of the parameters was increased. Increasing the number of *k*-points from $4 \times 4 \times 1$ to $6 \times 6 \times 1$ in the Monkhorst–Pack scheme led to insignificant variations in the equilibrium geometry and the total energy, which indicated that the setup was sufficient to produce the correct energies for the cases tested in the present study [27].

3 Results

The adsorption energy, representing the interaction between Ca and the rutile TiO_2 surface, is derived according to the following equation:

$$E_{ads} = E_{(Ca+TiO_2\ surface)} - (E_{Ca} + E_{TiO_2\ surface}), \quad (1)$$

where $E_{(Ca+TiO_2\ surface)}$, E_{Ca}, and $E_{TiO_2\ surface}$ represent the total energy of the TiO_2 surface with Ca adsorption, the energy of the Ca atom only, and the energy of the hydroxylated TiO_2 surface only. E_{Ca} was calculated by placing a single Ca atom in the middle of a largeish unit cell and computing the total energy. The more negative the E_{ads}, the more stable the adsorbed structure. Table 1 lists the binding energy of Ca adsorption on different surfaces. All of the E_{ads} were negative, which indicated that all four surfaces, even the bare R(110) surface, can induce Ca adsorption. The ability of rutile surfaces to induce Ca adsorption, including a bare rutile surface without any modification, is consistent with previous reports [10, 12]. The R(110) surface covered with OH had almost the same adsorption energy as the bare R(110) surface while the R(110) surface with exposed oxygen had the highest adsorption energy. These results imply that ability of a hydroxylated Ti surface to adsorb Ca may be less than that of an oxidized Ti surface, which contradicts the perception that large amounts of OH groups are beneficial to inducing apatite in SBF.

During the adsorption process, the Ca atoms induce a surface atom rearrangement that mainly involves the distortion of the geometry of the bridging O atoms and the OH groups on the surfaces. Geometric rearrangement due to metal atom adsorption has also been reported when the Pd atom interact with the R(110) surface [28]. Comparisons of the configurations of the top layers before and after Ca adsorption might help us to visualize the roles of the OH groups and water molecules in the adsorption process. In Case 3, the distance between the surface O and 5f-Ti changed very little before (1.69 Å) and after (1.71 Å) Ca adsorption (Fig. 3). However, the distance between O_{OH} and 5f-Ti on the surface increased from 1.90 Å to 2.32 Å after Ca adsorption in Case 2 (Fig. 2). In case 4, before Ca adsorption, the distance between O_{water} and 5f-Ti was 2.20 Å and the distance between the O_{OH} and 5f-Ti was 1.96 Å.

Table 1 Adsorption energy between different titanium oxide surfaces and the Ca atom. (unit: eV)

	Substrates	$E_{(Ca+TiO_2\ surface)}$	$E_{TiO_2\ surface}$	E_{Ca}	E_{ads}
Case 1	Bare rutile 110 surface	−19970.60	−18967.65	−999.64	−3.32
Case 2	Rutile 110 surface with OH	−20909.88	−19906.55	−999.64	−3.69
Case 3	Rutile 110 surface with O	−20846.00	−19835.77	−999.64	−10.59
Case 4	Rutile 110 surface with mixed OH and water	−20910.47	−19906.81	−999.64	−4.02

After Ca adsorption, these distances changed to 3.19 Å and 2.78 Å, respectively. Thus, it can be speculated that the hydroxyl groups and water tend to detach from the rutile surface and bind to the Ca atoms during the adsorption process, which in turn prevents Ca from adsorbing on the rutile surface. This configuration analysis suggests that the OH that is loosely bonded to 5f-Ti may be not beneficial to Ca adsorption while the OH formed from hydrogenated bridging oxygen bonding tightly with 6f-Ti does help in Ca adsorption.

The electron density configuration gives us an intuitive physical picture of Ca adsorption. Figure 6 shows the three-dimensional isosurface plot of the electron density with a value of 0.2 e/Å^3. The selected isosurface has been colored according to the magnitude of the gradient of the total density to emphasize the regions associated with bonding interactions, which allows one to distinguish the formation of a bonding interaction between the Ca atoms and rutile surfaces [28]. The electron densities of Ca atoms and oxygen atoms are found to overlap along the Ca–O direction (Fig. 6a, c). However, the electron density isosurface shows the repulsion between Ca and hydrogen with Ca adsorption on the fully hydroxylated surface and the mixed water surface (Fig. 6b, d). The electron density configuration demonstrates that the oxygen atoms play a positive role during Ca deposition while hydrogen atoms might has negative effects. The electron density difference maps clearly show the electron transfer during adsorption. The electron density difference ($\Delta\rho$) was calculated by subtracting the electron density of the isolated Ca (ρ_{Ca}) and surfaces ($\rho_{Surface}$) from the total electron density of the system ($\rho_{Ca+Surface}$) according to the following equation:

$$\Delta\rho = \rho_{Ca+Surface} - (\rho_{Ca} + \rho_{Surface}). \quad (2)$$

This equation produces a density difference field that indicates the changes in the electron distribution resulting from Ca adsorption. The field appropriately illustrates the valence electron redistribution due to chemical bonding. Figure 7 shows the electron density difference slices passing through the Ca and two bridging atoms. The charge accumulation and charge depletion are shown in red and blue, respectively. Clearly, there is charge accumulation near the oxygen atoms and charge depletion near the Ca along the Ca–O direction. This indicates that there is charge transfer from Ca to oxygen and a chemical bond between them is formed.

To understand the nature of the bonds of adsorbed Ca on rutile surfaces, detailed analyses of the electron structure on the basis of the density of state were carried out. The total density of state (TDOS) and the partial density of states (PDOS) of Ca adsorption on fully hydroxylated R(110) (Case 2) are shown in Fig. 8. Antibonding above the Fermi level comes mainly from Ti3d and Ca4s and partially from H2s in the energy range of 0–4 eV. The PDOS of the Ca3d and O2p, as well as the Ca2p and O2s have overlapping peaks. We may thus expect substantial hybridization between the Ca3d and O2p. The DOS results demonstrated that the main bonding occurs between Ca and

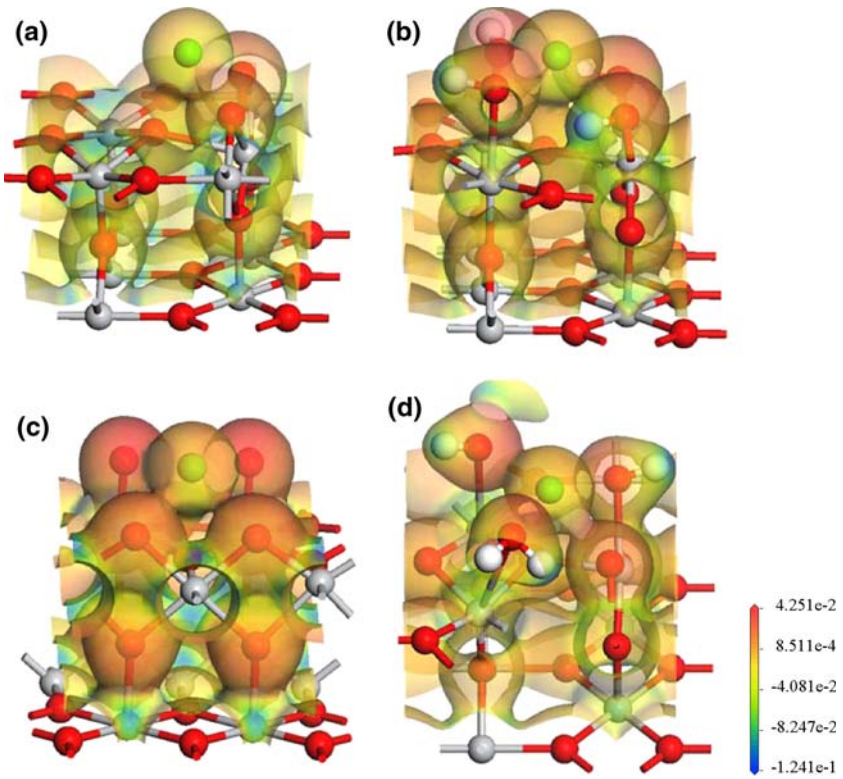

Fig. 6 A three-dimensional isosurface plot of the electron density with an iso value of 0.2 e/Å^3. **a** Ca on bare R(110) surface; **b** Ca on fully hydroxylated surface, which shows the repelling effect between Ca and H atoms; **c** Ca on fully oxidized surface, which shows an overlap between Ca and O atoms; **d** Ca on mixed water surface

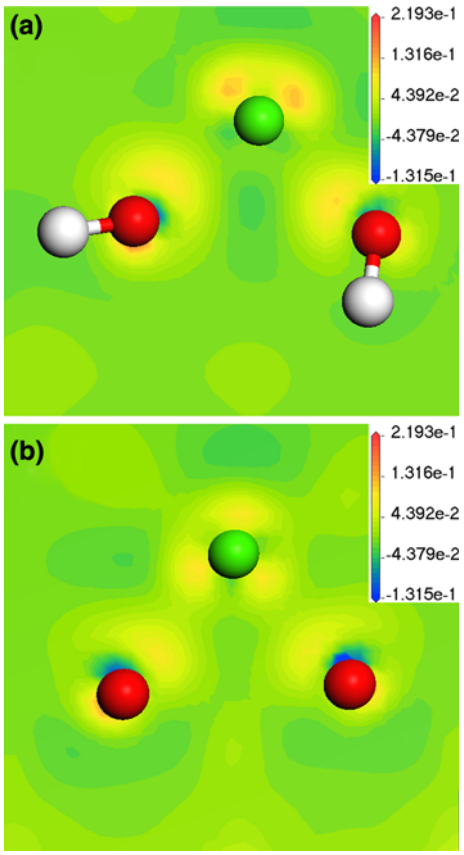

Fig. 7 Electron density difference slices passing through Ca and two bridging O atoms. The charge accumulation and charge depletion are represented by red and blue, respectively. **a** Case 2; **b** Case 3. (Color figure online)

O, which is consistent with the electron density analysis results.

Population analysis is helpful in understanding electron transfers and interactions among different atoms during Ca adsorption on TiO_2 surfaces. Population analysis is performed by using a projection of the plane wave states onto a localized basis set, and the resulting projected states are then analyzed using the Mulliken formalism [29]. The overlapping populations between the Ca atoms and atoms on rutile surfaces are given in Table 2. A large positive value indicates that the atoms are bonded; a large negative value indicates the atoms are in an antibonded state; a value close to zero indicates that there is no significant interaction between the electron populations of the two atoms [30]. As in Case 1, the overlapping population between Ca and O5 and O6 were found to be relatively high (0.13), which indicates a high degree of covalency in the bonds between O5–Ca and O6–Ca. There is also a weak bond between O10 and Ca. On the other hand, the overlapping population between Ca and Ti8 was found to be −0.59 while those between Ca and H were found to be $-0.03 \sim -0.06$. In Case 3, there are strong bonds between Ca and the oxygen atoms, including the bridging oxygen atoms (O5 and O6) and the oxygen atoms connected to the 5f-Ti sites (O15 and O16). In Cases 2 and 4, there exist antibonding interactions between Ca and hydrogen. The population analysis revealed that the bond between Ca and oxygen is the main factor affecting Ca adsorption.

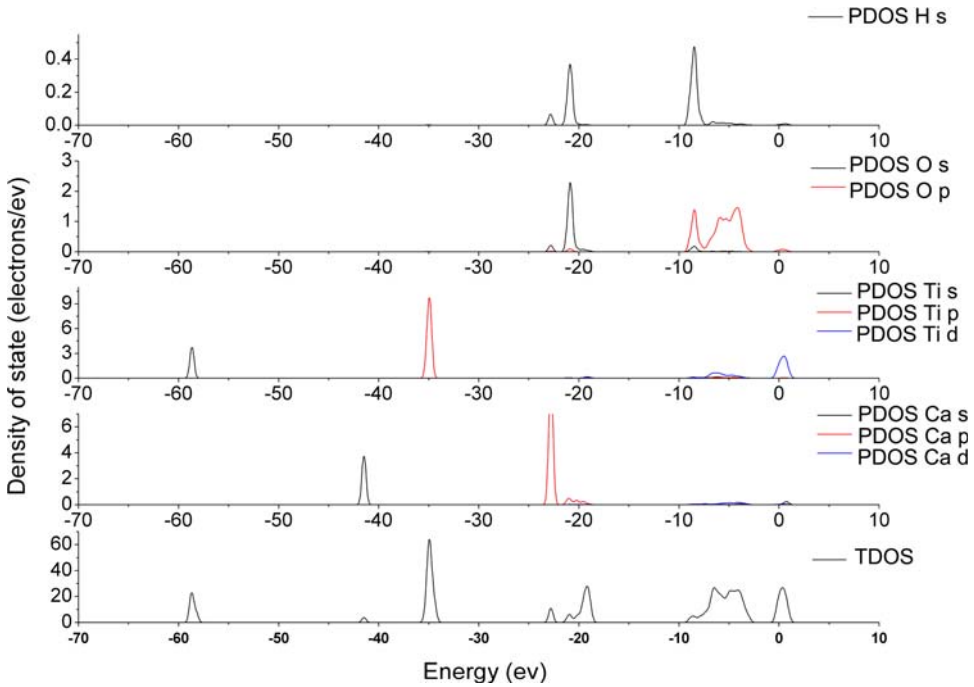

Fig. 8 The total density of state (TDOS) and partial density of states (PDOS) of Ca adsorption on the fully hydroxylated R(110) surface

Table 2 Bond population and the distances of atoms on the top of TiO_2 surfaces after Ca adsorption for atomic distances less than 3.5 Å

	Case 1		Case 2		Case 3		Case 4	
	Population	Distance	Population	Distance	Population	Distance	Population	Distance
O5–Ca	0.13	2.15	0.04	2.46	0.06	2.44	0.09	2.36
O6–Ca	0.13	2.15	0.06	2.39	0.06	2.40	0.08	2.37
O10–Ca	0.04	2.24	0.04	2.38	0.01	2.40	0.05	2.27
O15–Ca	–	–	0.19	2.17	0.16	2.20	0.19	2.24
O16–Ca	–	–	0.18	2.21	0.16	2.20	0.11	2.35
Ti3–Ca	–	–	−0.05	3.36	−0.05	3.08	−0.05	3.47
Ti4–Ca	–	–	−0.05	3.41	−0.05	3.08	–	–
Ti8–Ca	−0.59	2.92	−0.05	3.17	−0.08	3.03	−0.11	3.07
H1–Ca	–	–	−0.02	2.33	–	–	–	–
H2–Ca	–	–	−0.02	2.25	–	–	−0.01	3.02
H3–Ca	–	–	−0.03	3.04	–	–	−0.06	2.80
H4–Ca	–	–	−0.03	2.85	–	–	−0.02	3.28
H5–Ca	–	–	–	–	–	–	−0.06	2.47

Mulliken charges were examined to analyze the value of electrons transferring before and after Ca adsorption on rutile surfaces (Table 3). The absolute magnitudes of atomic charges have little physical meaning because of their sensitivity to the chosen basis set. However, their relative values can yield useful information about the bonding. In all cases, the net charges of the oxygen atoms increase after Ca adsorption, especially the bridging oxygen atoms (O5 and O6). In Case 3, the oxygen atoms connected to the 5f-Ti sites (O15 and O16) exhibit the largest gains in charge, which indicates a charge transfer from the Ca to the oxygen atoms and probably leads to a partial ionic contribution to the Ca–O bonding. Both the Ti and hydrogen atoms lose charges during the adsorption process, which reveals a weak antibonding interaction between Ca, Ti and H atoms. The Mulliken charge analysis demonstrated that the electron transfer determined by the electron density analysis is reasonable. By combing the population analysis and Mulliken charge calculations, we can reason that the OH group does not attract Ca adsorption and both the Ti and hydrogen atoms on the surface hinder Ca adsorption.

4 Discussion

Bioactive orthopedic materials are defined as materials capable of developing a direct, adherent, and strong bonding with the bone tissue. A bioactive implant should conduct or induct bone-like apatite growth on its surface when implanted in a living body and it should bond to bone through this apatite layer. Various materials were examined for their apatite-forming abilities in SBF. Gels of SiO_2 and TiO_2 are effective in inducing apatite formation because there are abundant OH groups on their surfaces [31]. Thus, the bioactivity of a titanium surface could be simply evaluated by the surface OH density [32]. However, a recent investigation on apatite formation on Ti surfaces with various types of treatments indicated that a heat-treated Ti surface with low OH concentration demonstrated better apatite formation than did an acid-etched surface although the acid-etched surface had a higher OH concentration than the heat-treated surface had [7]. This study was motivated by the following question: what is the role of OH groups in the apatite formation? A subsequent question is what material surface favors bone-like apatite formation.

4.1 OH group effects

It is well documented that titanium oxide surfaces have amphoteric OH, half of the OH groups are acidic in character, the other half are mainly basic [33, 34]. Thanks to computer simulation, we are able to investigate the roles of different types of OH in the Ca adsorption process. In our models, two types of OH groups can be easily identified: those bound to 5f-Ti and those formed by bridging oxygen atoms (Fig. 2). OH bound to the 5f-Ti is singly coordinated to one Ti and has a tendency to dissociate as a whole from the surface, which shows weak basic properties. On the other hand, OH formed by the bridging oxygen atoms are doubly coordinated to two Ti atoms and these bridging oxygen atoms are strongly polarized by Ti atoms that loosen the bond to hydrogen atoms. These OH groups have a strong tendency to release H and show predominately basic properties. The amphoteric characteristics of OH on

Table 3 Mulliken charges of atoms on the top of TiO_2 surfaces

	Case 1			Case 2			Case 3			Case 4		
	Before Ca adsorption	After Ca adsorption	Δe	Before Ca adsorption	After Ca adsorption	Δe	Before Ca adsorption	After Ca adsorption	Δe	Before Ca adsorption	After Ca adsorption	Δe
Ca		0.98			1.3			1.34			1.34	
O5	−0.59	−0.74	0.15	−0.76	−0.81	0.05	−0.54	−0.67	0.13	−0.78	−0.85	0.07
O6	−0.59	−0.74	0.15	−0.76	−0.83	0.07	−0.54	−0.68	0.14	−0.63	−0.73	0.1
O9	−0.70	−0.71	0.01	−0.65	−0.71	0.06	−0.69	−0.7	0.01	−0.67	−0.71	0.04
O10	−0.70	−0.77	0.07	−0.65	−0.73	0.08	−0.69	−0.72	0.03	−0.68	−0.75	0.07
O13	−0.70	−0.71	0.01	−0.69	−0.68	−0.01	−0.68	−0.72	0.04	−0.66	−0.7	0.04
O14	−0.70	−0.7	0.00	−0.69	−0.69	0.00	−0.68	−0.69	0.01	−0.68	−0.7	0.02
O15	–	–	–	−0.81	−0.89	−0.08	−0.35	−0.61	0.26	−0.85	−0.98	0.13
O16	–	–	–	−0.81	−0.94	−0.13	−0.35	−0.61	0.26	−0.83	−0.91	0.08
Ti3	1.36	1.2	−0.16	1.37	1.27	−0.1	1.28	1.21	−0.07	1.38	1.19	−0.19
Ti4	1.36	1.2	−0.16	1.37	1.21	−0.16	1.29	1.2	−0.09	1.38	1.21	−0.17
Ti7	1.27	1.24	−0.03	1.36	1.29	−0.07	1.31	1.29	−0.02	1.31	1.25	−0.06
Ti8	1.27	1.19	−0.08	1.36	1.19	−0.17	1.31	1.18	−0.13	1.32	1.14	−0.18
H1	–	–	–	0.39	0.31	−0.08	–	–	–	–	–	–
H2	–	–	–	0.39	0.31	−0.08	–	–	–	0.40	0.37	−0.03
H3	–	–	–	0.42	0.38	−0.04	–	–	–	0.42	0.42	0.00
H4	–	–	–	0.42	0.41	−0.01	–	–	–	0.43	0.43	0.00
H5	–	–	–	–	–	–	–	–	–	0.41	0.40	−0.01

TiO_2 surfaces have been demonstrated in our simulation. As shown in Case 2, the distance between the oxygen in hydroxyl and 5f-Ti on the surface increased from 1.91 to 2.33 after Ca adsorption, which means that the basic-site OH prefers to dissociate from the surface and bonds with Ca to form a Ca–OH complex. The main attraction between the Ca and TiO_2 surface is from the double-coordinated acid OH group. This argument is further demonstrated in Case 3, in which all the deprotonated oxygen atoms are strongly bonded to Ca and they do not prefer to leave the surface as the distance between the oxygen atoms and surface almost does not change. Our study is similar to that of Svetina et al., in which FPMD simulations were used to investigate the adsorption of Ca to identify the electrostatic interaction between the Ca complexes and negatively charged deprontonated sites as the main driving force of Ca adsorption [16]. This analysis could be used to explain our previous experimental results that heat-treated surfaces with low OH concentration have better apatite formation than do acid-etched surfaces, although the acid-etched surfaces have a higher OH concentration [7]. The reason might be that not all OH groups on acid-etched surfaces are strongly bonded with Ti and the weakly absorbed OH groups may be not beneficial to Ca adsorption. The heat treatment removed a large amount of weakly adsorbed water molecules on the titanium surface and therefore made it conducive to apatite formation.

4.2 Water effects

Water adsorption on the R(110) surface affects Ca adsorption. The nature of water adsorption on an ideal R(110) surface is still a controversial issue although considerable efforts have been devoted to it [13, 20]. Water molecules may fully dissociate into H and OH or partially dissociate and exist as water molecules on the R(110) surface. To clarify the effects of water, we used a mixed model, water molecules coexisting with OH groups, which have been proved to energetically stable according to previous reports [13, 21]. After geometric optimization, the oxygen in the water molecule (O_w) was bound to the 5f-Ti with a bond length of 2.20 Å, and one of the water's hydrogen atoms formed a hydrogen bond with one of the bridging O-atoms (Fig. 4b). This result is consistent with the report of Langel using the CPMD package [20], which indicates that our modeling is reasonable and also that the calculation accuracy is acceptable. In the next step, a Ca atom was put on the surface. After the calculation, the water departed from the surface and had a tendency to combine with the Ca atoms (Fig. 4d). The distance between O_w and Ti was 3.19 Å while the distance between O_w and Ca was 2.35 Å. The population analysis revealed that the bond population of O_w–Ti was 0.03 and that of O_w–Ca was 0.19, which indicates that the interaction of O_w–Ca was much stronger than that of O_w–Ti and the

water molecules weakly adsorbed on Ti had the tendency to bind with Ca. Another interesting finding in the mixed model is that the distance of OH–(5f-Ti) in Case 4 (2.78 Å, Fig. 4d) was larger than that in Case 2 (2.32 Å, Fig. 2b), which indicates that the existence of water molecules also influences the adjacent OH bonding states since the adjacent OH groups also increase the tendency to depart from the surface. The effects of the water molecules on Ca adsorption suggest that a certain kind of treatment to remove water molecules from surfaces, such as heat treatment or alkaline treatment, would be helpful to apatite formation.

4.3 Hydrogen effects

Our simulation findings could be used to explain why hydrogen titanate cannot induce apatite formation. According to the recent report of Kokubo [31], when titanium is subjected to NaOH solution and then to HCl solution, hydrogen titanate is formed on the titanium surface. The hydrogen titanate does not induce apatite information on the titanium surface in SBF. However, when the titanium is subsequently subjected to heat treatment to form titanium oxide, apatite formation is induced on the titanium surface in SBF. The mechanism leading to no apatite formation on hydrogen titanate could be interpreted in terms of the hydrogen atoms on the titanium surface. After being soaked in HCl solution, NaOH-treated titanium releases all the Na ions and is converted to hydrogen titanate, which in turn introduces a large number of hydrogen atoms on the surface. As analyzed in the previous sections, hydrogen and Ca repel each other and hydrogen precludes Ca adsorption on the surface. As a result, the ability to form apatite on the titanium surface is lost. However, when the NaOH and HCl-treated titanium surfaces were heat-treated, the hydrogen titanate on the surface is converted to anatase and rutile, and hence the surface obtains the apatite formation ability.

It is should be borne in mind that the apatite formation process, especially the precursory stages, is very complex and still not well understood yet. This study has sought to model the effects of OH groups on calcium adsorption, which is the very first step in apatite formation. It is found that part of OH and water dissociates from the surface and combine with Ca. In the later stage, the formation of an ion-rich, gel-like layer could be a necessary step in apatite formation. Further study is needed to investigate how OH groups are incorporated in apatite nucleation. Another important point is that these models present a simplified picture of Ca adsorption without considering other factors in the real condition, such as water and proteins. The study of proteins and water effects on Ca adsorption probably requires molecular dynamic methods due to large computational cost of DFT methods [15].

5 Conclusions

Our first-principles quantum mechanics calculations indicate that all types of rutile (110) surfaces, including bare surfaces without any molecular groups, surfaces with full OH groups, surfaces with full O atoms, and surfaces with water molecules and OH groups, can bond with Ca ions. R(110) surfaces covered with oxygen atoms have the highest ability to attract Ca ions, which partially explains why alkali-treated Ti surfaces can induce apatite formation in alkali environments. Not all OH groups help to attract Ca adsorption and hydrogen atoms on the surface hinder Ca adsorption. Loosely bonded OH and water actually combine with Ca and certain treatments that remove the water molecules on the surfaces such as heat treatments or alkaline treatments should be helpful to apatite formation. This study of the relationship between OH groups and Ca adsorption advances our understanding of the bioactivity mechanism by modifying titanium surfaces. The findings in this study have potential impact on the design of effective surface treatments of metals for bioactivity enhancement.

Acknowledgements This project was financially supported by the NSFC (30700172), NSFC/RGC Joint Research Funding (N_HKUST 601/08, 30831160509), Specialized Research Fund for the Doctoral Program of Higher Education for Young Teacher (20070613019), and National Key Project of Scientific and Technical Supporting Programs Fund from MSTC (2006BAI16B01).

References

1. Lu X, Zhao Z, Leng Y. Biomimetic calcium phosphate coatings on nitric-acid-treated titanium surfaces. Mater Sci Eng C. 2007; 27:700–8.
2. Kokubo T, Kim H, Kawashita M. Novel bioactive materials with different mechanical properties. Biomaterials. 2003;24:2161–75.
3. Kokubo T, Kim HM, Kawashita M, Nakamura T. Bioactive metals: preparation and properties. J Mater Sci: Mater Med. 2004;15: 99–107.
4. Kokubo T, Miyaji F, Kim H, Nakamura T. Spontaneous formation of bonelike apatite layer on chemically treated titanium metals. J Am Ceram Soc. 1996;79:1127–9.
5. Lu X, Leng Y. TEM study of calcium phosphate precipitation on bioactive titanium surfaces. Biomaterials. 2004;25:1779–86.
6. Lu X, Leng Y. Theoretical analysis of calcium phosphate precipitation in simulated body fluid. Biomaterials. 2005;26:1097–108.
7. Lu X, Wang Y, Yang X, Zhang Q, Zhao Z, Weng L, et al. Spectroscopic analysis of titanium surface functional groups under various surface modification and their behaviors in vitro and in vivo. J Biomed Mater Res. 2008;84A:523–34.
8. Segall MD, Lindan PJD, Probert MJ, Pickard CJ, Hasnip PJ, Clark SJ, et al. First-principles simulation: ideas, illustrations and the CASTEP code. J Phys Condens Matter. 2002;14(11):2717–43.
9. Clark SJ, Segall MD, Pickard CJ, Hasnip PJ, Probert MJ, Refson K, et al. First principles methods using CASTEP. Zeitschrift fuer Krystallographie. 2005;220:567–70.
10. Rohanizadeh R, Al-Sadeq M, LeGeros RZ. Preparation of different forms of titanium oxide on titanium surface: effects on apatite deposition. J Biomed Mater Res. 2004;71A:343–52.

11. Uchida M, Kim HM, Kokubo T, Fujibayashi S, Nakamura T. Structural dependence of apatite formation on titania gels in a simulated body fluid. J Biomed Mater Res. 2003;64A:164–70.
12. Wang XX, Yan W, Satoshi H, Tsuru K, Osaka A. Apatite deposition on thermally and anodically oxidized titanium surfaces in a simulated body fluid. Biomaterials. 2003;24:4631–7.
13. Harris LA, Quong AA. Molecular chemisorpiton as the theoretically preferred pathway for water adsorption on ideal rutile TiO_2(110). Phys Rev Lett. 2004;93:0861051–4.
14. Pabisiak T, Kiejna A. Energetics of oxygen vacancies at rutile TiO_2(110) surface. Solid State Commun. 2007;144:324–8.
15. Kornherr A, Tortschanoff A, Portuondo-Campa E, van Mourik F, Chergui M, Zifferer G. Modelling of aqueous solvation of eosin Y at the rutile TiO_2(110)/water interface. Chem Phys Lett. 2006; 430:375–9.
16. Svetina M, Ciacchi LC, Sbaizero O, Meriani S, DeVita A. Deposition of calcium ions on rutile (110): a firstprinciples investigation. Acta Mater. 2001;49:2169–77.
17. Komolov AS, Moller PJ, Mortensen J, Komolov SA, Laznev EF. Modification of the electronic properties of the TiO_2 (110) surface upon deposition of the ultrathin conjugated organic layers. Appl Surf Sci. 2007;253:7376–80.
18. San Miguel MA, Oviedo J, Sanz JF. Ca deposition on TiO_2(110) surfaces: insights from quantum calculations. J Phys Chem C. 2009;113(9):3740–5.
19. Bates SP, Kresse G, Gillan MJ. The adsorption and dissociation of ROH molecules on TiO_2(110). Surf Sci. 1998;409:336–49.
20. Langel W. Car-Parrinello simulation of H_2O dissociation on Rutile. Surf Sci. 2002;496:141–50.
21. Lindan PJD, Harrison NM, Gillan MJ. Mixed dissociative and molecular adsorption of water on the rutile (110) surface. Phys Rev Lett. 1998;80:762–5.
22. Han Y, Liu CJ, Ge QF. Interaction of Pt clusters with the anatase TiO_2(101) surface: a first principles study. J Phys Chem B. 2006; 110:7463–72.
23. Ding K, Li J, Zhang Y. Cu and NO coadsorption on TiO_2(110) surface: a density functional theory study. J Mol Struc-Theochem. 2005;728:123–7.
24. Mattsson A, Leideborg M, Larsson K, Westin G, Osterlund L. Adsorption and solar light decomposition of acetone on anatase TiO_2 and niobium doped TiO_2 thin films. J Phys Chem B. 2006; 110:1210–20.
25. Vanderbilt D. Soft self-consistent pseudopotentials in a generalized eigenvalue formalism. Phys Rev B. 1990;41:7892–5.
26. Monkhorst HJ, Pack JD. Special points for Brillouin-zone integrations. Phys Rev B. 1976;13:5188–92.
27. Zhang Z, Fenter P, Kelly SD, Catalano JG, Bandura AV, Kubicki JD, et al. Structure of hydrated Zn^{2+} at the rutile TiO_2 (110)-aqueous solution interface: comparison of X-ray standing wave, X-ray absorption spectroscopy, and density functional theory results. Geochimica Cosmochimica Acta. 2006;70:4039–56.
28. Sanz JF, Marquez A. Adsorption of Pd atoms and dimers on the TiO_2 (110) surface: a first principles study. J Phys Chem C. 2007;111:3949–55.
29. Long R, Dai Y, Jin H, Huang B. Structural, elastic, and electronic properties of ReB2: a first-principles calculation. Res Lett Phys. 2008;Article ID 293517:1-5.
30. Segall MD, Shah R, Pickard CJ, Payne MC. Population analysis of plane-wave electronic structure calculations of bulk materials. Phys Rev B. 1996;54(23):16317–20.
31. Kokubo T, Matsushita T, Takadama H, Kizukia T. Development of bioactive materials based on surface chemistry. J Euro Ceram Soc. 2009;29:1267–74.
32. Feng B, Weng J, Yang BC, Qu SX, Zhang XD. Characterization of surface oxide films on titanium and adhesion of osteoblast. Biomaterials. 2003;24:4663–70.
33. Boehm H. Acidic and basic properties of hydroxylated metal oxide surface. Faraday Discuss. 1971;52:264–75.
34. Sham T, Lazarus M. X-ray photoelectron spectroscopy studies of clean and hydrated TiO_2 surfaces. Chem Phys Lett. 1979;68:426–32.